Cell Metabolism
Article

Dissecting Multiple Steps of GLUT4 Trafficking and Identifying the Sites of Insulin Action

Li Bai,[1,4] Yan Wang,[1,4] Junmei Fan,[1,4] Yu Chen,[1] Wei Ji,[1] Anlian Qu,[2] Pingyong Xu,[1,*] David E. James,[3] and Tao Xu[1,2,*]
[1] Joint Laboratory of Institute of Biophysics and Huazhong University of Science and Technology, National Laboratory of Biomacromolecules, Institute of Biophysics, Chinese Academy of Sciences, Beijing 100101, China
[2] College of Life Science and Technology, Huazhong University of Science and Technology, Wuhan 430074, China
[3] Diabetes and Obesity Program, Garvan Institute of Medical Research, Sydney 2010, Australia
[4] These authors contributed equally to this work.
*Correspondence: pyxu@moon.ibp.ac.cn (P.X.), xutao@ibp.ac.cn (T.X.)
DOI 10.1016/j.cmet.2006.11.013

SUMMARY

Insulin-stimulated GLUT4 translocation is central to glucose homeostasis. Functional assays to distinguish individual steps in the GLUT4 translocation process are lacking, thus limiting progress toward elucidation of the underlying molecular mechanism. Here we have developed a robust method, which relies on dynamic tracking of single GLUT4 storage vesicles (GSVs) in real time, for dissecting and systematically analyzing the docking, priming, and fusion steps of GSVs with the cell surface in vivo. Using this method, we have shown that the preparation of GSVs for fusion competence after docking at the surface is a key step regulated by insulin, whereas the docking step is regulated by PI3K and its downstream effector, the Rab GAP AS160. These data show that Akt-dependent phosphorylation of AS160 is not the major regulated step in GLUT4 trafficking, implicating alternative Akt substrates or alternative signaling pathways downstream of GSV docking at the cell surface as the major regulatory node.

INTRODUCTION

Insulin-stimulated transport of glucose into muscle and fat cells is mediated by the redistribution of the insulin-responsive glucose transporter GLUT4 (Birnbaum, 1989; James et al., 1988) from intracellular GLUT4 storage vesicles (GSVs) to the plasma membrane (PM) (Bryant et al., 2002). The insulin-stimulated redistribution of GLUT4 involves the insulin signal transduction and vesicle trafficking pathways, each of which is comprised of multiple steps. Despite recent progress in our understanding of insulin signaling and GLUT4 trafficking, the convergence point between these two pathways has yet to be defined. A major limitation is that it is not known which step (or steps) in the GLUT4 trafficking pathway is regulated by insulin. This could include budding of GSVs from intracellular compartments (Karylowski et al., 2004; Watson et al., 2004); transport of vesicles along microtubules and cortical actin (Bose et al., 2002; Thurmond et al., 2003; Semiz et al., 2003); and/or docking, priming, and then fusion of vesicles at the PM (Bryant et al., 2002; Bose et al., 2004; Satoh et al., 1993). Although the insertion of GLUT4 into the PM can be assessed by extracellular epitope labeling of GLUT4 (Czech et al., 1993) and by conventional membrane fractionation assays (Robinson et al., 1992), there is a great need for higher-resolution methods that can distinguish the multiple steps of GSV trafficking prior to fusion.

Extensive efforts have been made to identify the insulin signaling pathways leading to the PM translocation of GLUT4. It is now well established that activation of PI3K through the insulin receptor substrate is essential for insulin-stimulated GLUT4 translocation (Saltiel and Kahn, 2001). Activation of PI3K is transmitted through PDK and its downstream target Akt/PKB. Recently, a substrate of Akt has been identified, AS160, that functions in GLUT4 trafficking (Sano et al., 2003). AS160 possesses a Rab GAP (GTPase-activating protein) domain, and thus it may regulate the activity of a Rab protein that is involved in GLUT4 trafficking. AS160 is phosphorylated at four separate sites by Akt. It has previously been shown that overexpression of an AS160 mutant (AS160-4P) in which each of these phosphorylation sites has been mutated inhibits insulin-stimulated GLUT4 translocation in adipocytes (Sano et al., 2003). In addition to the Akt pathway, other signaling intermediates have been implicated in the insulin-dependent regulation of GLUT4 trafficking. These include the atypical PKC ζ/λ isoform (Bandyopadhyay et al., 2002) and a novel signaling pathway involving CAP/Cbl/TC10 (Chiang et al., 2001). Despite this knowledge, the steps along the GLUT4 trafficking pathway at which PI3K and AS160 act as well as the interplay between the Akt and the alternative pathways described above remain to be demonstrated. In vitro reconstitution assays have been used to implicate the PM as an important target for insulin/Akt action in GLUT4 trafficking (Koumanov et al., 2005). However, these assays were unable to resolve discrete steps in GLUT4 trafficking including docking, priming, and fusion.

Table 1. Summary of Kinetic Analysis of GSV Docking and Fusion

		Vesicle Density (μm^{-2})	Docking Rate (10^{-3} $\mu m^{-2} \times s^{-1}$)	Fusion Rate (10^{-3} $\mu m^{-2} \times s^{-1}$)	Mean Dwell Time (s)	k_2/k_{-1}	$k_1(s^{-1})$	$k_{-1}(s^{-1})$	$k_2(s^{-1})$
Control (n = 5)	Control	0.52 ± 0.06	2.28 ± 0.35	0.035 ± 0.012	6.1 ± 0.061	0.0156	4.38×10^{-3}	0.155	0.0024
	Insulin	0.63 ± 0.03	4.15 ± 1.06	0.28 ± 0.06	4.2 ± 0.04	0.0724	6.59×10^{-3}	0.222	0.016
Wortmannin (n = 6)	Control	0.56 ± 0.07	0.38 ± 0.14	NA	NA	NA	0.68×10^{-3}	NA	NA
	Insulin	0.62 ± 0.09	0.20 ± 0.06	NA	NA	NA	0.32×10^{-3}	NA	NA
AS160-4P (n = 4)	Control	0.52 ± 0.06	1.04 ± 0.39	NA	NA	NA	2.00×10^{-3}	NA	NA
	Insulin	0.54 ± 0.09	0.78 ± 0.26	NA	NA	NA	1.44×10^{-3}	NA	NA

Vesicle density was measured as the number of mobile vesicles identified in the TIRF zone divided by the area of the footprint of each cell. The docking/fusion rate was defined as the number of docking/fusion events divided by the footprint area of each cell and the duration of the imaging series (100 s, in our case), respectively. The mean dwell time was obtained by fitting the exponential decay time constant of the dwell time distribution as shown in Figure 4D. For Scheme 1, the mean dwell time is expected to equal $1/(k_{-1} + k_2)$ (Colquhoun and Hawkes, 1995). The k_2/k_{-1} ratio was calculated as fusion rate/(docking rate − fusion rate). From these data, we were able to derive the rate constants (k_1, k_2, and k_{-1}) of Scheme 1. n = number of cells analyzed; the number of docking vesicles analyzed per cell was 30–50 on average.

The evanescent field generated by total internal reflection fluorescence microscopy (TIRFM) selectively illuminates fluorophores within a thin layer underneath the PM (Lang et al., 1997) and thus images only the footprint where the cell adheres to the coverslip. Previous studies have demonstrated that EGFP-tagged GLUT4 can be used to visualize single GSVs under TIRFM in adipocytes (Li et al., 2004a; Lizunov et al., 2005). The study by Lizunov et al. provided an elegant demonstration of the use of TIRFM for studying GLUT4 trafficking in adipocytes and showed that insulin has an important action at the PM. However, in that study, a detailed kinetic analysis of the different steps that comprise the encounter and fusion of GSVs with the PM was not undertaken, and so it remains unclear whether there is one key regulated step or multiple regulated steps. This would represent a major breakthrough in this area, facilitating future efforts to connect the insulin signaling and vesicle transport pathways. In the present study, we have used TIRFM to study the trafficking of EGFP-tagged GLUT4 in 3T3-L1 adipocytes. In view of the stochastic nature of the behavior of GLUT4 vesicles, a rigorous interrogation of this process will require the acquisition and analysis of a considerable amount of morphological data. To overcome this hurdle, we have developed a computational method in MATLAB to analyze time-lapse images of GLUT4 trafficking in a semiautomated fashion. Using this approach, we have analyzed thousands of events in adipocytes incubated in the absence or presence of insulin. We have been able to dissect the GLUT4 trafficking process into several discrete steps including docking, priming, and fusion and to measure the transition kinetics between these steps. To our knowledge, this has not been previously reported for this particular biological process. A detailed quantitative analysis of this process revealed that insulin accelerates two steps at the PM that underpin GLUT4 translocation. The first involves vesicle docking, and the second is a step that prepares GLUT4 vesicles for fusion competence after docking at the PM. Quantitative kinetic analysis of these events revealed that the postdocking step is the major regulated step. Moreover, by combining imaging analysis with either drugs that interfere with the function of PI3K or overexpression of a mutated version of the Rab GAP AS160, we were able to conclude that the docking step is regulated by PI3K and its downstream effector AS160. These studies raise the possibility that the major insulin-regulated step at the PM that controls GLUT4 translocation either is an Akt-independent step or involves a target of Akt that has yet to be described.

RESULTS

Identifying Docking and Fusion of GSVs

Using time-lapse imaging under TIRFM at a frame rate of 5 Hz, we observed the movement of numerous fluorescent particles in 3T3-L1 adipocytes transfected with GLUT4-EGFP, as demonstrated in Movie S1 in the Supplemental Data available with this article online. We occasionally observed fusion of these fluorescent particles with the PM, and the fusion events were upregulated by insulin (see Table 1), suggesting that these EGFP-labeled subplasmalemmal vesicles are functionally competent GSVs that are insulin responsive. Figure 1A displays images of a GSV fusing with the PM. Radial sweeps were calculated for each image and could be fitted well with Gaussian functions. As shown in Figure 1A, the amplitude of the Gaussian fit first increases followed by a fast decay. Concomitantly, the width of the Gaussian fit (δ) increases as GLUT4 diffuses laterally in the PM after fusion. By placing two concentric circles centered at the fusion site, we could observe the diffusion of GLUT4-EGFP into the annulus between the two circles, which results in a significant increase in fluorescence followed by an exponential decay within the annulus (Figure 1B). The diffusion of GLUT4-EGFP away from the site of GSV fusion at the PM was regarded as diffusion from a point source in a plane

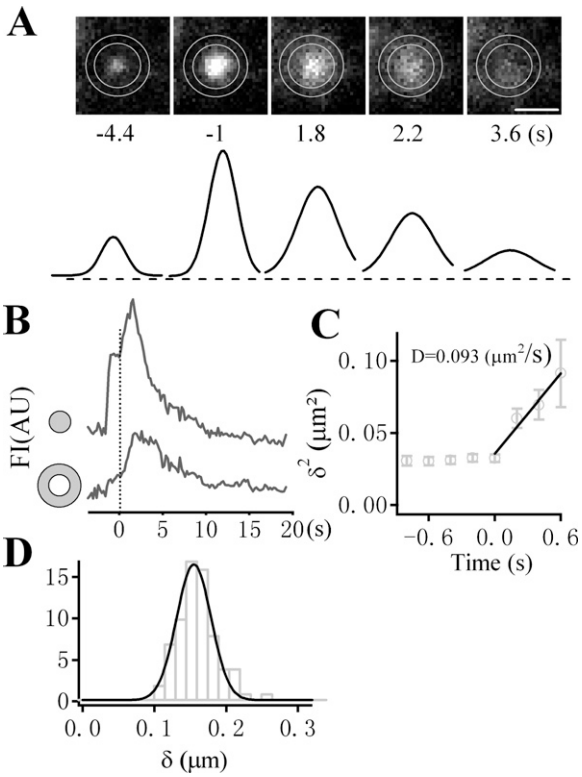

Figure 1. Labeling GLUT4 Storage Vesicles in Adipocytes

(A) TIRFM images of a GLUT4 storage vesicle (GSV) fusing with the PM under insulin stimulation. Times indicated are relative to the onset of fusion. Gaussian fits of the radial fluorescence profile (in arbitrary units) of the vesicles for each image are plotted underneath. Scale bar = 1 μm.

(B) Time courses of the fluorescence intensity (FI) in arbitrary units (AU) in the inner circle and the annulus centered at the GSV. The inner circle and the annulus are depicted in (A) with a diameter of ~1.0 and ~1.3 μm, respectively. Significant increase in the annular fluorescence is observed after fusion, followed by exponential decay, which indicates diffusion of fluorescence (GLUT4-EGFP) from the fusion site.

(C) Time course of δ^2, the square of the width of the Gaussian fits for fusion of GSVs. The line is a best fit to the points at t > 0 s, weighted inversely by the square of their error bars (±SEM). The slope corresponds to a diffusion coefficient of 0.093 $\mu m^2/s$.

(D) Size distribution of 70 fusing GSVs. The width of the Gaussian fits, δ, was used as a measure of the size. Smooth line is the Gaussian fit of the distribution with a peak of 155 nm.

(Crank, 1970), thus allowing us to determine the diffusion coefficient (D) according to the equation $\delta^2 = D \times t$. We estimated the diffusion coefficient to be 0.093 $\mu m^2/s$ (Figure 1C). The diffusion coefficient is about ten times less than the reported value for lipid dyes such as FM1-43 (1.2 $\mu m^2/s$) (Zenisek et al., 2002) or Di-I (1.0–1.4 $\mu m^2/s$) (Jacobson et al., 1981) but is comparable to the values reported for membrane proteins (Lizunov et al., 2005; Schmoranzer et al., 2000). The much slower diffusion of GLUT4-EGFP in the PM is advantageous for quantifying GSV fusion events. The size of fusion-competent GSVs (gauged by δ from 2D Gaussian fit) reveals a single Gaussian distribution with a peak at ~155 nm (Figure 1D). Based on this size distribution, we restricted our analysis to fluorescent particles where δ < 268 nm, which will include more than 99% of the vesicles that follow the size distribution.

For a penetration depth of the evanescent field of 113 nm in our setup, the density of membrane-proximal vesicles of the footprint in the absence and presence of stimulation (100 nM insulin for 2 min) was 0.52 ± 0.06/μm^2 and 0.63 ± 0.03/μm^2 (n = 5 cells), respectively, which is significantly higher than that reported from primary rat adipocytes (Lizunov et al., 2005). This number represents the time average of the number of spots in a time series of images. Most of the GSVs underneath the PM are in active motion, particularly in the z direction, as demonstrated in Movie S1. The majority of GSVs traveled primarily via random or constrained diffusion, as reported for secretory granules (Steyer et al., 1997; Oheim and Stuhmer, 2000), whereas a small fraction (~3%) of vesicles traveled in a directed fashion, as if along a preformed track. We next set out to experimentally define the docking step of GSVs with the PM. Most vesicles rapidly appeared and disappeared in the evanescent field, giving the impression that they are constantly sampling or bombarding the PM (see examples indicated by square in Movie S1). We also frequently observed vesicles that approached the PM perpendicularly or at a steeper angle and then remained static at that site for a defined period while maintaining a relatively constant level of fluorescence. We have analyzed several hundred vesicles that exhibit this behavior, which we defined as docking. One example is shown in Figure 2A (see also Movie S2). The vesicle was invisible at the beginning of the sequence and then abruptly appeared, attaining a nearly constant level of fluorescence. The vesicle then remained stationary in the lateral plane, indicating that it had been immobilized at a site within the PM. The vesicle oscillated slightly in the z axis, as manifested by the fluctuating fluorescence (Figure 2B). In contrast to the fusion event in Figure 1, we did not observe any increase of fluorescence in the annular area (Figure 2B). We calculated the 3D displacement ($R^{(3)}$) of a vesicle and defined a docking event if its $R^{(3)}$ was <0.067 μm (the size of one pixel) for ten consecutive frames. Often we observed that docked vesicles vanished from the evanescent field without spreading or diffusion of the fluorescence as shown in Figure 1, suggesting that the vesicle had undocked from the PM rather than undergone fusion. We developed a semiautomated method to detect and analyze these docking events. In general, from a stack of 500 images (100 s) with ~200 identified GSVs in each image, we identified ~100 docking events at a docking rate of (2.28 ± 0.35) × 10^{-3} $\mu m^{-2} \times s^{-1}$ in unstimulated cells.

Kinetic Analysis of the Docking and Fusion Steps

To analyze the kinetics of the docking process, we measured the dwell time that GSVs spent in the docked state, which is defined as the time interval between docking and undocking (Figure 2B). Construction of the distribution of the dwell time from a large number of events is necessary to assess the stochastic behavior of the docking state. It is

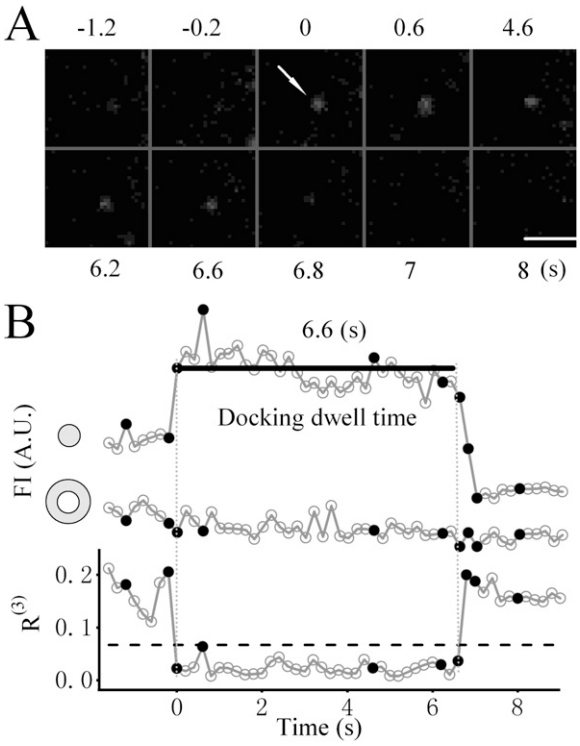

Figure 2. Docking and Undocking of GSVs with the PM

(A) Sequential images of a single GSV from an unstimulated cell as it approaches and docks at the PM and then undocks without fusion after 6.6 s. Times indicated are relative to the beginning of docking. Arrow indicates the position of docking. Scale bar = 1 μm. See time course in (B) for more information. Real-time images of this vesicle are presented in Movie S2.

(B) Time courses of the fluorescence intensity (FI) in arbitrary units (AU) from the inner and annular area and the 3D displacement ($R^{(3)}$; see Experimental Procedures) from the docking site for the vesicle shown in (A). The fluorescence intensity in the annulus remained stable as displayed, which is indicative of an undocking event without fusion with the PM. Horizontal dashed line marks the level of 0.067 μm, which we used as a threshold to identify docking. The duration below this threshold (indicated by two vertical dotted lines) measures the docking dwell time. Filled circles indicate the time points of the images in (A).

anticipated that the docking of GSVs at the PM might be a thermodynamic process; hence, the docking dwell time should be temperature dependent. To demonstrate this, we compared the GSV docking kinetics in cells maintained at different temperatures. As shown in Figure 3A, the distribution of the dwell time follows a single-exponential decay at any given temperature, suggesting that our definition of docking includes only one kinetic state. In Figure 3B, we compared the cumulative distributions of the dwell time at different temperatures under basal conditions. For the exponentially distributed data set, the mean dwell time equals the exponential time constant of its distribution. We found that the mean dwell time is substantially reduced with increased temperature, with an estimated Q_{10} of −6.6 (inset, Figure 3B). These data indicate that increased temperature reduces the time that GSVs spend in the docked state, possibly by enhancing the undocking rate. This result emphasizes the importance of maintaining constant temperature when analyzing the kinetics of vesicular docking and fusion. Subsequent experiments were thus carried out at precisely 30°C.

Having defined the docking state, we next asked whether there is an intermediate state between docking and fusion. To this end, we analyzed the interval between the initial GSV docking event and subsequent fusion with the PM. In the absence of insulin, the spontaneous fusion rate was as low as $0.035 \pm 0.01\ \mu m^{-2} \times s^{-1}$. Strikingly, insulin caused a substantial increase in the fusion rate (see Table 1), demonstrating the robust insulin responsiveness of our experimental system. Figure 4A displays a typical fusion event in an insulin-stimulated cell. As shown in Figure 4B, a discernible docking stage was observed prior to fusion. The vesicle gradually brightened as it approached the PM, accompanied by a decrease in its mobility. It then immobilized at a given site with 3D displacement less than 0.067 μm for 23 consecutive frames (4.6 s). Suddenly the vesicle fused with the PM, as indicated by a significant increase of fluorescence in the annular area, which manifests the gradual diffusion of fluorescence from the point of vesicle docking. Our ability to clearly distinguish vesicle docking and vesicle fusion at the PM allowed us to quantify a third parameter, fusion latency, as the interval between docking and fusion (marked with two vertical dashed lines in Figure 4B and plotted as a histogram in the inset of Figure 4C). It should be noted that the construction of the fusion latency histogram does not require identification of the docking step in advance. In some cases, we observed fusion events with no identifiable docking state, suggesting a transient docking time less than our sampling interval (200 ms). These events were characterized by a docking time of <0.2 s and were included in the first bin (0–1 s) in the distribution histogram of fusion latency. The histogram of fusion latency displays a monoexponential decay and is identical to the cumulative distribution of the docking dwell time of undocked vesicles from the same batch of cells (Figure 4C). Thus, the immobilized state that we describe above represents the same docking state, regardless of whether the vesicle subsequently undocks or fuses.

We thus propose a simple model as shown in Scheme 1 that consists of a linear sequence of reversible states followed by an irreversible fusion reaction. In this simple model, we start with a pool of mobile vesicles (MVs) that are located at a distance of <200 nm from the PM, or two times the penetration depth of the evanescent field (Oheim and Stuhmer, 2000). These peripheral MVs have been described both in 3T3-L1 adipoctyes (Oatey et al., 1997) and primary adipose cells (Malide et al., 2000) and have been suggested to be the carriers of GLUT4 in response to insulin stimulation. The MVs are highly mobile and are constantly screening the PM for docking. Once the MVs dock at the PM, they become docked vesicles (DVs). We defined the transition rate constant from MVs to DVs as k_1. DVs can either fuse with the PM at a rate constant of k_2 or undock at an undocking rate constant of k_{-1}.

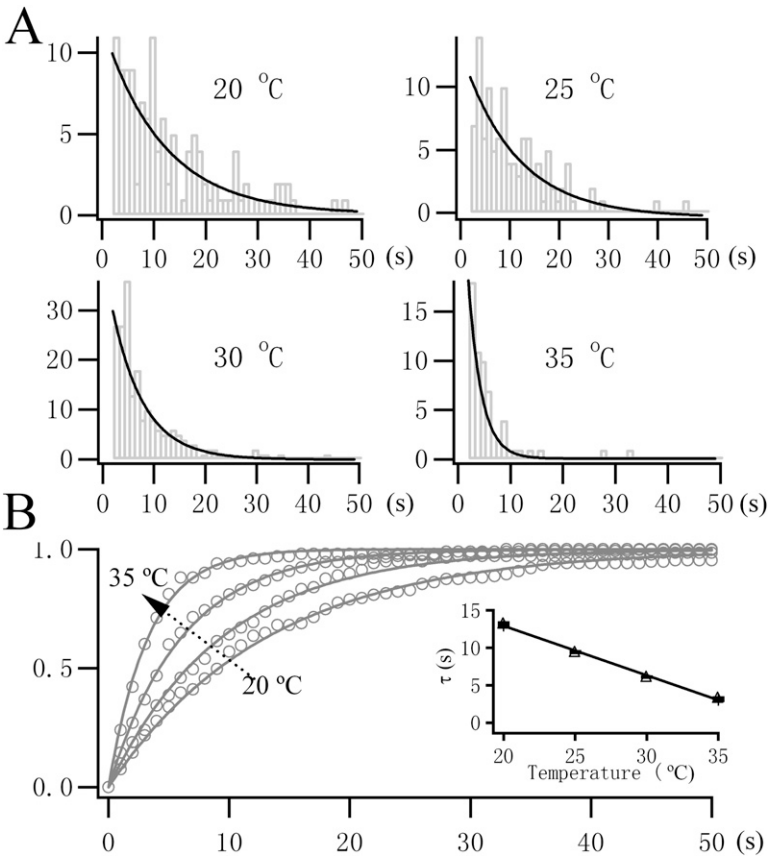

Figure 3. Temperature Dependence of the Docking Kinetics

(A) Distributions of the docking dwell time at four different temperatures in the base state. Superimposed smooth lines represent the exponential fit of the distribution. The numbers of vesicles analyzed are 122, 109, 198, and 58 for 20°C, 25°C, 30°C, and 35°C, respectively.

(B) Comparison of the cumulative distribution of the docking dwell time from 20°C to 35°C. Dotted arrow indicates the direction of increasing temperature. Superimposed smooth lines are the single-exponential fits to the cumulative distribution. The time constants (τ) of the distributions were obtained from each fit and plotted against temperature in the inset. The line fit in the inset estimates the temperature dependence of τ. Data at each temperature were collected from 3–4 cells.

$$\mathrm{MV} \underset{k_{-1}}{\overset{k_1}{\rightleftharpoons}} \mathrm{DV} \xrightarrow{k_2} \mathrm{Fusion} \qquad \text{Scheme 1}$$

Identifying the Key Steps Regulated by Insulin

One of the major questions in GLUT4 trafficking is which step (or steps) is regulated by insulin. Insulin could recruit more GSVs to the DV state by increasing k_1, stabilize GSVs in the DV state by decreasing the undocking rate constant k_{-1}, or increase the fusion of DVs by increasing k_2. To directly test these possibilities, we solved the kinetic parameters as depicted in Scheme 1 by comparing the kinetics of GSVs in the absence and presence of insulin from the same batch of cells. From Scheme 1, we infer that the dwell time in the docking state (DV) should follow a single-exponential distribution with a time constant (τ) equal to $1/(k_{-1} + k_2)$ (Colquhoun and Hawkes, 1995). We can also count the number of fusion and undocking events and calculate the ratio between them to estimate k_2/k_{-1}. The docking rate should be the product of MV and k_1. Hence, we are able to solve all of the kinetic parameters shown in Scheme 1. At early times after insulin addition (2–3 min), we observed only a slight increase (~21%) in the density of MVs in the evanescent field. At later times after insulin addition (~20–30 min), however, the density of MVs was decreased, presumably because a significant number of GSVs had already fused with the PM (see Figure 5A). This is consistent with the study by Lizunov et al. (2005). Insulin increased the docking rate by ~2-fold and increased the fusion rate by ~8-fold (see Table 1). Figure 4D compares the cumulative distribution of docking dwell time for basal and insulin-treated conditions. Insulin resulted in a significant reduction in the mean dwell time, from 6.1 ± 0.061 s to 4.2 ± 0.04 s ($p < 0.029$ by Mann-Whitney test). From these data, we were able to calculate the rate constants shown in Scheme 1 and show that insulin has a major effect on k_2, increasing this parameter by 6-fold (Table 1). Insulin also increased k_1 by 1.5-fold. Hence, these data indicate that a key insulin-regulated step is the step after docking at the PM, perhaps a priming step enabling the docked vesicles to become fusion competent.

Pinpointing the Site of Action of PI3K and Its Downstream Effector AS160

Taking advantage of our ability to dissect these different stages of GLUT4 trafficking using TIRFM, we next attempted to define the point of action of PI3K since this signaling intermediate has been shown to play an important regulatory role in GLUT4 trafficking (Tengholm and Meyer, 2002). To accomplish this, cells were incubated with the PI3K inhibitor wortmannin prior to TIRF analysis. As shown in Figure 5, insulin caused a time-dependent increase in cell-surface GLUT4-EGFP levels, reaching a new steady state by 20 min. This is consistent with the time course for insulin-stimulated GLUT4 translocation reported in

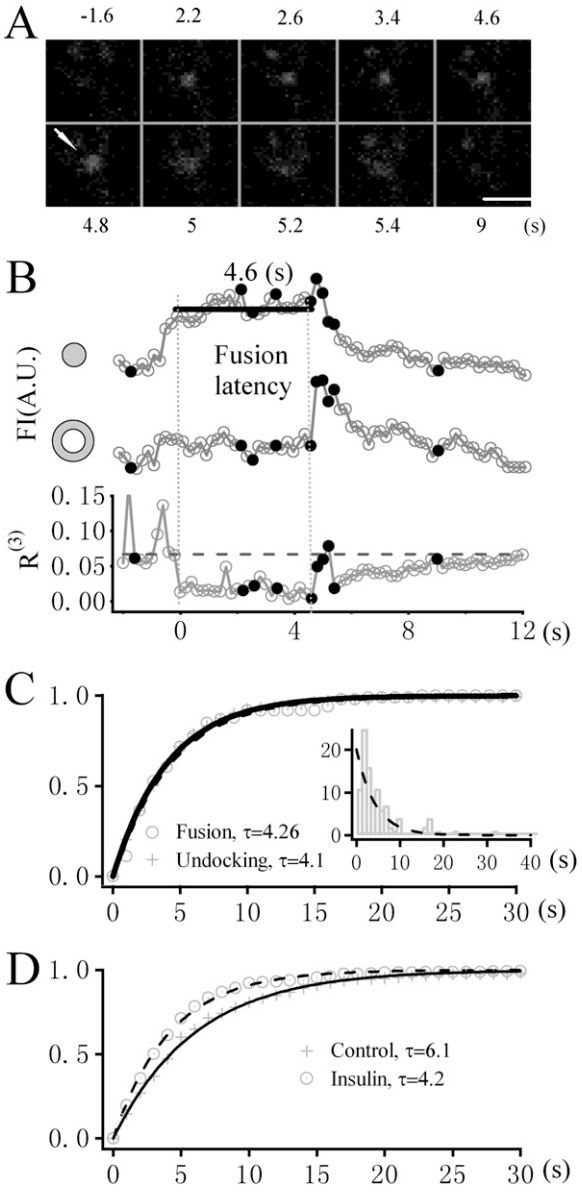

Figure 4. Insulin Shortens the Dwell Time in the Docked State

(A) Docking often precedes membrane fusion. Sequential images of a single GSV as it approaches and then docks at the PM for 4.6 s and undergoes fusion with the PM are shown. (See also Movie S3.) Times indicated are relative to the beginning of docking. Arrow indicates the position of fusion. Scale bar = 1 μm.

(B) Time course of the fluorescence intensity (FI) in arbitrary units (AU) in the inner circle and the annular area and the 3D displacement ($R^{(3)}$) for the vesicle shown in (A). Horizontal dashed line marks the level of 0.067 μm. The increase of fluorescence intensity in the annular area exceeds three times the standard deviation of the prefusion stage, which we used as a criterion to define fusion. The second vertical dotted line marks the time of fusion, and the duration between two vertical dotted lines measures the fusion latency after docking. Filled circles indicate the time points of the images in (A).

(C) The cumulative distribution of the fusion latency is indistinguishable from the docking dwell time for undocked events collected from the same batch of cells at 30°C. All the data were collected in the presence of insulin because spontaneous fusion events in the absence of insulin are rare. Single-exponential fits to the two cumulative distributions are superimposed and are indistinguishable, with time constants of 4.26 s (n = 100 vesicles) and 4.1 s (n = 207 vesicles) for fusion and undocking events, respectively. The distribution of the fusion latency is displayed as a histogram in the inset, which is fitted by an exponential decay with a time constant of 4.3 s (dashed line).

(D) Comparison of the cumulative distribution of docking dwell time in the absence (Control, n = 273 vesicles) and presence of insulin (Insulin, n = 421 vesicles). Dashed lines are single-exponential fits to the corresponding cumulative distribution. Insulin reduced the time constant τ from 6.1 s to 4.2 s. The two data sets are significantly different as determined by Mann-Whitney test ($p < 0.029$) or Kolmogorov-Smirnov test ($p < 0.026$).

other studies (Tengholm and Meyer, 2002; Govers et al., 2004). While some studies (Bogan et al., 2001; Holman et al., 1994) have reported a more rapid rate of increase, it is relevant to point out that the present studies were conducted at 30°C rather than 37°C. Wortmannin completely inhibited insulin-dependent GLUT4 translocation to the PM, consistent with previous studies (Clarke et al., 1994; Kotani et al., 1995; Okada et al., 1994). Analysis of individual docking events revealed that wortmannin had no significant effect on the movement of GSVs toward the PM, as determined by measurement of the density of MVs in the evanescent field. Surprisingly, stabilized docking of GSVs was almost completely absent in the presence of wortmannin. Rather, mobile GSVs were visible for only a few frames, as if they briefly entered the evanescent field and sampled the PM but were unable to be captured at this location. Quantitation of this effect revealed that wortmannin reduced the docking rate by 95% with insulin stimulation and 83% without insulin stimulation (see Table 1).

AS160 is a downstream effector of PI3K that plays an important role in GLUT4 trafficking (Sano et al., 2003) with an unidentified site of action. To determine the site of action of AS160, we overexpressed wild-type AS160 and its dominant-negative mutant, AS160-4P, in adipocytes. We found that the overexpressed wild-type AS160 protein only slightly impaired insulin-dependent GLUT4 trafficking, whereas the overexpressed AS160-4P mutant caused a 75% reduction in insulin-stimulated translocation of GLUT4-EGFP in adipocytes (Figure 5C), consistent with previous results (Sano et al., 2003). The density of MVs was not significantly reduced by AS160-4P (Table 1). Interestingly, overexpression of AS160-4P caused a significant inhibition in the docking rate (Figure 5E; Table 1), an effect similar to that observed with wortmannin. The cumulative distribution of dwell time from residual docking events after AS160-4P blockade is indistinguishable from that of control cells (data not shown), suggesting that AS160 is probably not involved in the steps downstream of docking.

DISCUSSION

The insulin regulation of GLUT4 translocation in muscle and fat cells is considered to represent a form of regulated exocytosis (Bryant et al., 2002). As is the case for other

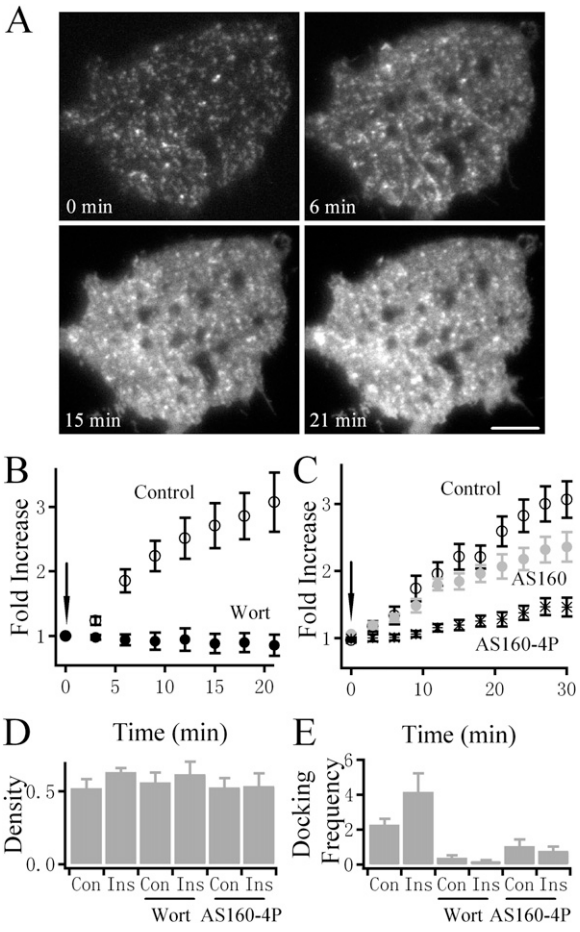

Figure 5. Docking Requires Activation of PI3K and AS160 Phosphorylation

(A) Insulin stimulates the insertion of GLUT4-EGFP into the basal PM. TIRFM images of the footprint of the same adipocyte at different times after insulin perfusion are shown. Scale bar = 5 μm.

(B) Time course of the change in fluorescence induced by insulin within the evanescent field in control (n = 10 cells) and wortmannin-treated (Wort; 100–200 nM, n = 6 cells) adipocytes. Fluorescence was normalized to the value prior to insulin application (indicated by arrow). Error bars in (B)–(E) represent ±SEM.

(C) Evanescent-field fluorescence increase induced by insulin (arrow indicates application) is blocked by transfection of AS160-4P (n = 12 cells). Overexpression of wild-type AS160 (n = 6 cells) exerts only a slight inhibition.

(D) Summary of the density (μm^{-2}) of subplasmalemmal GSVs from control cells, cells treated with wortmannin (20 min), and cells overexpressing AS160-4P.

(E) The averaged docking rate (in 10^{-3} $\mu m^{-2} \times s^{-1}$) is increased by insulin ($p = 0.05$, Student's t test) but is dramatically reduced by wortmannin ($p < 0.01$) and AS160-4P overexpression ($p < 0.05$).

regulated secretory events, it is thought that the GLUT4 translocation process is the end result of a complex series of steps culminating in the fusion of the intracellular GLUT4 storage vesicles (GSVs) with the PM. Despite this, it has not been feasible to experimentally resolve most of these steps, particularly those close to the PM, due to technical limitations. This is a major problem in the field because it is still not known which step or steps within this process are regulated by insulin. One method that has the potential to resolve the GLUT4 translocation process into its component steps is TIRFM. This method has recently been employed to study GLUT4-EGFP trafficking in 3T3-L1 fibroblasts (Li et al., 2004a), 3T3-L1 adipocytes (Gonzalez and McGraw, 2006), and primary rat adipocytes (Lizunov et al., 2005). While these studies have advanced our understanding of the process, they have been somewhat limited because individual vesicular trafficking events were not analyzed in detail and the conclusions were for the most part based upon indirect measurements. For example, Gonzalez and McGraw measured changes in cell-surface GLUT4 fluorescence versus membrane-proximal fluorescence using TIRF in response to insulin and concluded that insulin's major effect was to increase GSV docking. However, it is not clear whether the fluorescence increase in the TIRF zone measured in that study is due to an increase of GLUT4 inserted in the PM or an increase in docked/recruited vesicles in the TIRF zone. Indeed, due to the complex equilibrium between docking, fusion, and endocytosis of GLUT4, as well as the nonlinear behavior of fluorescence in the TIRF zone due to the exponential decay of excitation power, it is hard to infer any effect on steps other than membrane insertion simply by measuring steady-state fluorophore-labeled GLUT4 under TIRFM. In the study of Lizunov et al. (2005), individual GSV docking and fusion events were described. However, in view of the limited data set, they did not conduct a rigorous kinetic analysis of their data, and their fusion rates were derived from steady-state equations with multiple assumptions. Nevertheless, these studies have highlighted the potential of TIRFM for resolving individual steps in the GLUT4 trafficking pathway, provided that the technique is combined with dynamic tracking and analysis of single GLUT4 vesicles.

In the current study, we have developed an approach to dissect and systematically analyze the docking, priming, and fusion steps of GSVs in live adipocytes. Detailed kinetic analysis of the stochastic behavior of a large number of GSVs has allowed us to define the major kinds of vesicular movement beneath the PM and how these vesicles interact with the PM. We found that most docking vesicles approach the PM perpendicularly or at a steeper angle, as previously reported for the docking of large dense core vesicles from chromaffin cells (Oheim and Stuhmer, 2000). This is in contrast to the report of Lizunov et al. (2005), in which GLUT4 vesicles often underwent long-range lateral movements prior to tethering. It is also noteworthy that we have defined a higher density of vesicles in the TIRF plane (~500 vesicles per 1000 μm^2 area) compared to that of Lizunov et al. (~160 vesicles per 1000 μm^2 area; Lizunov et al., 2005). Whether these differences in movement and density reflect differences between primary rat adipocytes and differentiated 3T3-L1 adipocytes is not presently clear. Regardless, the system we describe in the present study is robust and has enabled us to systematically analyze the kinetics of docking and fusion of GSVs with the PM. Using this approach, we have

identified two major insulin-regulated steps at the PM. The first involves vesicle docking with the PM. This step is only slightly modified by insulin, is regulated by PI3K, and appears to be the target of the Rab GAP AS160. The second step, which appears to be the key insulin-regulated step, is proximal to vesicle docking and precedes vesicle fusion. Our results demonstrate a striking increase (~6-fold) induced in the fusion rate constant of docked GSVs by insulin. These data lay the foundation to explore the role of a number of different molecules already implicated in GLUT4 trafficking in more detail. For example, the exocyst complex and the myosin motor protein Myo1c have been shown to play a role in the initial encounter of GSVs with the PM (Bose et al., 2002; Saltiel and Pessin, 2003). It should now be feasible to determine whether they are involved in the docking step described in the present studies. This step likely brings GSVs sufficiently close to the PM to facilitate assembly of the SNARE complex. In the case of GLUT4 trafficking, this involves the vesicular SNARE VAMP-2 and the plasma membrane SNAREs syntaxin 4 and SNAP-23 (James, 2005). Since insulin dramatically accelerates a priming step after docking, it is possible that the formation of the SNARE complex is a key molecular event regulated by insulin during this priming step. It is conceivable that in resting adipocytes, syntaxin4 is masked by interacting proteins such as Munc18c, precluding its interaction with VAMP-2 on the GSVs (Kanda et al., 2005). Hence, a key regulated target in insulin signaling could act to increase the availability of free syntaxin 4 or the conformation of syntaxin 4 such that it can then form productive SNARE complexes. The assembly of the SNARE complex will further bring the GSV membrane into close proximity to the PM and initiate subsequent fusion (Jahn et al., 2003; Sorensen, 2005). Obviously, much of this model is based upon studies of other SNARE complexes in other systems (Jahn et al., 2003). However, the TIRF system described here should provide a way forward to test the role of these and other molecules in GLUT4 trafficking with more definition than has been possible in the past.

In this study, we have made several important observations. First, the appearance of GLUT4 vesicles just beneath the PM was not the major effect of insulin. In view of the proximity of GSVs with respect to the PM even under basal conditions, this is perhaps not surprising. Some studies have suggested that there is an insulin-responsive, wortmannin-insensitive step that facilitates the transport of vesicles out toward the cortex of the cell (Bogan et al., 2001; van Dam et al., 2005). One possibility is that this step delivers vesicles to a region outside the evanescent field, rendering it difficult to visualize by TIRFM. It is notable that microtubules have been reported to facilitate the delivery of GSVs to the cell surface, and this step may well terminate in the vicinity of the PM (Huang et al., 2005). Regardless, because expression of constitutively active versions of either Akt or PI3K is sufficient to trigger GLUT4 translocation (Tengholm and Meyer, 2002; Kohn et al., 1998), it seems unlikely that this wortmannin-insensitive step plays a major role in insulin action.

Second, we have found that, while insulin accelerates GSV docking, significant docking of GSVs is also evident in the absence of insulin, and the addition of wortmannin almost completely abolished this process (Figure 5). These data suggest that activation of a wortmannin-sensitive PI3K even under basal conditions is required to maintain a threshold level of GSV docking. However, accelerated docking and subsequent fusion require insulin signaling. This hypothesis is consistent with recent experiments demonstrating that GSV accumulation underneath the cell surface requires only a submaximal insulin concentration (1 nM) and that fusion requires higher insulin concentrations (Kanda et al., 2005).

Third, we have demonstrated that overexpression of a dominant-negative AS160 mutant produces a reduction in GSV docking similar to wortmannin. This suggests that PI3K regulates docking through activation of Akt and its downstream substrate AS160. Specific Rab proteins and their effectors have been hypothesized to mediate the docking of vesicles at the target membrane (Jahn et al., 2003). Collectively, then, these data provide evidence that the cognate Rab protein of AS160 residing on GSVs likely participates in the docking of GSVs through interaction with a putative Rab effector at the PM.

Finally, our data provide evidence for an additional insulin-regulated step downstream of docking, and this step appears to be a major regulated step in the overall process of GLUT4 translocation. Because this step is distal to docking and because wortmannin inhibits docking, we are unable to determine the PI3K dependence of this step using the methodology described here. Regardless, this step likely involves a target of insulin action that is distinct from AS160, and future studies are needed to pinpoint its molecular identity. Koumanov et al. (2005) have reported an 8-fold increase in heterotypic fusion of intracellular GSVs with reconstituted PMs obtained from insulin-treated cells and identified the PM as the major target of insulin action. Our data are consistent with this finding, although their cell-free method cannot discriminate between docking and fusion. We believe that our study reinforces the notion that the PM is the major target of insulin action vis à vis GLUT4 trafficking and extends this model by showing that the major regulated step is distal to GSV docking with the PM. We propose that this step is controlled by the SNARE proteins themselves or a SNARE associated protein (or proteins).

Studies in neurons have identified numerous proteins that interact with the t-SNAREs syntaxin 1a and SNAP-25 (Jahn et al., 2003), and these molecules appear to play a key role in accelerated vesicle fusion. Very few syntaxin 4/SNAP-23-associated molecules have been identified in insulin-responsive cells, and we believe that future studies should be directed toward the identification of such molecules. Once identified, we propose that the system described in this study, in which it is feasible to dissect individual steps of GLUT4, should be the method of choice in further testing the function of such molecules in GLUT4 trafficking. The next major challenge will be to identify the signaling pathway that intersects with such

molecules and to determine whether it represents one of the known pathways, such as the Akt pathway, or an as yet unidentified pathway. In support of the latter, Kanda et al. (2005) have shown that adipocytes from Munc18c knockout mice display insulin-dependent but wortmannin-independent GLUT4 translocation, raising the possibility that an additional signaling pathway is required to drive the GLUT4 translocation process downstream of vesicle docking. It is intriguing that Munc18c and syntaxin 4 have recently been shown to undergo insulin-dependent phosphorylation in adipocytes (Schmelzle et al., 2006; Oh and Thurmond, 2006), and future studies will be required to examine the functional significance of these observations. The present studies emphasize the need for an intensive effort to unravel the molecular basis for this insulin-regulated step at the PM that controls GLUT4 translocation in adipocytes.

EXPERIMENTAL PROCEDURES

Cell Culture and Transfection

3T3-L1 cells were cultured in high-glucose DMEM (GIBCO) supplemented with 10% newborn calf serum (GIBCO) at 37°C and 5% CO_2. One day after confluence, the cells were switched into differentiation medium containing 10% fetal bovine serum (GIBCO), 1 μM bovine insulin, 0.5 mM 3-isobutyl-1-methylxanthine, and 0.25 μM dexamethasone. Two days later, the medium was changed with 10% fetal bovine serum and 1 μM bovine insulin for another two days. The cells were then maintained in DMEM with 10% fetal bovine serum. Seven days after differentiation, 3T3-L1 adipocytes were treated with 0.05% trypsin-EDTA (GIBCO) and washed twice with Opti-MEM (GIBCO) by centrifugation at 1500 rpm at room temperature. The cells were resuspended in Opti-MEM (GIBCO), and 40 μg GLUT4-EGFP (Li et al., 2004a) plasmid was added to a final volume of 800 μl. Cells were then electroporated at 360V for 10 ms using a BTX 830 electroporator (Biocompare) and plated on coverslips coated with poly-L-lysine. Experiments were performed two days after transfection in KRBB solution containing (in mM) 129 NaCl, 4.7 KCl, 1.2 KH_2PO_4, 5 $NaHCO_3$, 10 HEPES, 3 glucose, 2.5 $CaCl_2$, 1.2 $MgCl_2$, 0.1% BSA (pH 7.2). Prior to the imaging experiment, adipocytes were serum starved for at least 2 hr and transferred to a home-made closed perfusion chamber. Most experiments were performed at 30°C because preliminary studies at 37°C revealed significant illumination damage after long-term (~30 min) fluorescence imaging at the latter temperature. This was not the case at 30°C. Insulin was applied at a concentration of 100 nM throughout the study. Unless otherwise stated, all drugs were purchased from Sigma.

TIRFM Imaging Collection and Analysis

The TIRFM setup was constructed based on the prismless and through-the-lens configuration as previously described (Li et al., 2004a). The penetration depth of the evanescent field was estimated to be 113 nm by measuring the incidence angle with a prism (n = 1.518) by 488 nm laser beam.

Data Analysis

We developed a program for semiautomated analysis of GSV movement in MATLAB (The MathWorks).First, the raw images were processed with KNN (k-nearest neighbor, k = 9 from 25 neighbors) filter to restrain hotspot noise from the CCD. Second, the images were further low-pass filtered (cutoff spatial frequency 0.5) to remove high-frequency noise. We then determined the area of the cell footprint by edge detection. In order to enhance the edge contrast, we normally averaged a stack of 500 consecutive images. Further analysis was then carried out within the edge, and the area was used to calculate the vesicle density. Within the edge, there are black holes, suggesting the existence of lipid droplets, which were not included in the calculation of the density of vesicles. The distribution of GLUT4-EGFP fluorescence in the PM is normally not homogeneous and will impose different local background fluorescence in identifying single vesicles. We thus used the "opening by reconstruction" algorithm implemented in MATLAB to remove the diffused background fluorescence. Individual fluorescence particles were then automatically segmented based on analyzing the gray level distribution of all pixels. Identified particles were fitted with a 2D Gaussian function to obtain the peak location and width. Only particles with width (δ) of Gaussian fit smaller than 268 nm were included for further analysis (see size distribution of Figure 1D). We then linked every particle from frame to frame to obtain the trajectory of each particle. Particles that were immobile during the whole imaging period (100 s) were also excluded from further analysis. For identifying docking events, we selected vesicles that moved less than one pixel for more than five consecutive frames for subsequent scrutiny. The putative docked vesicles were then tracked by the 2D Gaussian fit-based algorithm written in MATLAB, which has proven effective in tracking single fluorescent particles at low signal-to-noise levels (Li et al., 2004b; Oheim and Stuhmer, 2000). The Gaussian peak was taken as the lateral position. The relative axial position was calculated as $Z_n = -d \ln(F_n)/(F_{max})$, where F_n is the background-subtracted fluorescence in frame n, d is the penetration depth, and F_{max} is the maximum fluorescence intensity (Oheim and Stuhmer, 2000). We calculated the 3D displacement as $R^{(3)} = ([x_n - x_0]^2 + [y_n - y_0]^2 + [z_n - z_0]^2)^{1/2}$, where (x_n, y_n, z_n) stands for the position of vesicle in frame n and (x_0, y_0, z_0) stands for the averaged position of the putative docking sites. We considered a docking event if $R^{(3)}$ was smaller than one pixel (0.067 μm) for more than ten consecutive frames. Since we only counted those GSVs that docked longer than ten consecutive images (2 s), we might have underestimated the docking events by missing a fraction equal to $\int_0^2 \tau * e^{(-t/\tau)} * dt$ of the events. Given a τ of 4.2 s for insulin-stimulated events, the missing fraction is 0.38 (38%). Because of this missing fraction, the mean dwell time was not determined by arithmetic averaging but rather by exponential fitting to its distribution.

To distinguish between fusion and undocking events, we measured radial fluorescence diffusion in the plasma membrane. To accomplish this, we placed two concentric circles (normally ~1.0 μm and ~1.3 μm in diameter, as illustrated in Figure 1A) centered at each vesicle being analyzed. We plotted the fluorescence within the inner circle and between the two circles (annulus). When there is fluorescence diffusion after fusion, we would expect a subsequent fluorescence increase in the annular area. When this fluorescence increase exceeded three times the standard deviation of the background fluorescence (see Figure 1B and Figure 4B), we defined this as a fusion event. In contrast, if the fluorescence within the annulus did not display a significant increase over the background, this was defined as an undocking event (see Figure 2B). Having identified these events, we tracked back to the first frame when the vesicle first arrived at the fusion site. This time was taken as the initial docking time. Another criteria imposed as a requirement for docking was that, during the interval between initial docking and fusion (or undocking), the vesicle remained immobilized ($R^{(3)}$ < 0.067 μm) in the TIRF zone.

Statistics

For normally distributed data, population averages are given as mean and standard error of mean (SEM) and statistical significance was tested using Student's t test. Statistical significance between exponential distributions was assessed using the Kolmogorov-Smirnov and Mann-Whitney tests.

Supplemental Data

Supplemental Data include three movies and can be found with this article online at http://www.cellmetabolism.org/cgi/content/full/5/1/47/DC1/.

ACKNOWLEDGMENTS

This work was supported by grants from the National Science Foundation of China (30470448, 30130230), the Major State Basic Research Program of China (2004CB720000, 2006CB0D1704), the CAS Project (KSCX2-SW-224, Y2004018), the Li Foundation, and the Sino-German Scientific Center. The laboratory of T.X. belongs to a Partner Group Scheme of the Max Planck Institute for Biophysical Chemistry (Göttingen, Germany). D.E.J. is a fellow of the National Health and Medical Research Council of Australia. We thank Dr. Gus Lienhard for providing AS160 cDNAs.

Received: August 21, 2006
Revised: October 17, 2006
Accepted: November 17, 2006
Published: January 2, 2007

REFERENCES

Bandyopadhyay, G., Sajan, M.P., Kanoh, Y., Standaert, M.L., Quon, M.J., Lea-Currie, R., Sen, A., and Farese, R.V. (2002). PKC-zeta mediates insulin effects on glucose transport in cultured preadipocyte-derived human adipocytes. J. Clin. Endocrinol. Metab. *87*, 716–723.

Birnbaum, M.J. (1989). Identification of a novel gene encoding an insulin-responsive glucose transporter protein. Cell *57*, 305–315.

Bogan, J.S., McKee, A.E., and Lodish, H.F. (2001). Insulin-responsive compartments containing GLUT4 in 3T3-L1 and CHO cells: regulation by amino acid concentrations. Mol. Cell. Biol. *21*, 4785–4806.

Bose, A., Guilherme, A., Robida, S.I., Nicoloro, S.M., Zhou, Q.L., Jiang, Z.Y., Pomerleau, D.P., and Czech, M.P. (2002). Glucose transporter recycling in response to insulin is facilitated by myosin Myo1c. Nature *420*, 821–824.

Bose, A., Robida, S., Furcinitti, P.S., Chawla, A., Fogarty, K., Corvera, S., and Czech, M.P. (2004). Unconventional myosin Myo1c promotes membrane fusion in a regulated exocytic pathway. Mol. Cell. Biol. *24*, 5447–5458.

Bryant, N.J., Govers, R., and James, D.E. (2002). Regulated transport of the glucose transporter GLUT4. Nat. Rev. Mol. Cell Biol. *3*, 267–277.

Chiang, S.H., Baumann, C.A., Kanzaki, M., Thurmond, D.C., Watson, R.T., Neudauer, C.L., Macara, I.G., Pessin, J.E., and Saltiel, A.R. (2001). Insulin-stimulated GLUT4 translocation requires the CAP-dependent activation of TC10. Nature *410*, 944–948.

Clarke, J.F., Young, P.W., Yonezawa, K., Kasuga, M., and Holman, G.D. (1994). Inhibition of the translocation of GLUT1 and GLUT4 in 3T3-L1 cells by the phosphatidylinositol 3-kinase inhibitor, wortmannin. Biochem. J. *300*, 631–635.

Colquhoun, D., and Hawkes, A.G. (1995). The principles of the stochastic interpretation of ion-channel mechanisms. In Single-Channel Recording, B. Sakmann and E. Neher, eds. (New York: Plenum Press), pp. 397–482.

Crank, J. (1970). The Mathematics of Diffusion (Oxford: Oxford University Press)., pp. 857–863.

Czech, M.P., Chawla, A., Woon, C.W., Buxton, J., Armoni, M., Tang, W., Joly, M., and Corvera, S. (1993). Exofacial epitope-tagged glucose transporter chimeras reveal COOH-terminal sequences governing cellular localization. J. Cell Biol. *123*, 127–135.

Gonzalez, E., and McGraw, T.E. (2006). Insulin signaling diverges into Akt-dependent and -independent signals to regulate the recruitment/docking and the fusion of GLUT4 vesicles to the plasma membrane. Mol. Biol. Cell *17*, 4484–4493.

Govers, R., Coster, A.C., and James, D.E. (2004). Insulin increases cell surface GLUT4 levels by dose dependently discharging GLUT4 into a cell surface recycling pathway. Mol. Cell. Biol. *24*, 6456–6466.

Holman, G.D., Lo, L.L., and Cushman, S.W. (1994). Insulin-stimulated GLUT4 glucose transporter recycling. A problem in membrane protein subcellular trafficking through multiple pools. J. Biol. Chem. *269*, 17516–17524.

Huang, J., Imamura, T., Babendure, J.L., Lu, J.C., and Olefsky, J.M. (2005). Disruption of microtubules ablates the specificity of insulin signaling to GLUT4 translocation in 3T3-L1 adipocytes. J. Biol. Chem. *280*, 42300–42306.

Jacobson, K., Hou, Y., Derzko, Z., Wojcieszyn, J., and Organisciak, D. (1981). Lipid lateral diffusion in the surface membrane of cells and in multibilayers formed from plasma membrane lipids. Biochemistry *20*, 5268–5275.

Jahn, R., Lang, T., and Sudhof, T.C. (2003). Membrane fusion. Cell *112*, 519–533.

James, D.E. (2005). MUNC-ing around with insulin action. J. Clin. Invest. *115*, 219–221.

James, D.E., Brown, R., Navarro, J., and Pilch, P.F. (1988). Insulin-regulatable tissues express a unique insulin-sensitive glucose transport protein. Nature *333*, 183–185.

Kanda, H., Tamori, Y., Shinoda, H., Yoshikawa, M., Sakaue, M., Udagawa, J., Otani, H., Tashiro, F., Miyazaki, J., and Kasuga, M. (2005). Adipocytes from Munc18c-null mice show increased sensitivity to insulin-stimulated GLUT4 externalization. J. Clin. Invest. *115*, 291–301.

Karylowski, O., Zeigerer, A., Cohen, A., and McGraw, T.E. (2004). GLUT4 is retained by an intracellular cycle of vesicle formation and fusion with endosomes. Mol. Biol. Cell *15*, 870–882.

Kohn, A.D., Barthel, A., Kovacina, K.S., Boge, A., Wallach, B., Summers, S.A., Birnbaum, M.J., Scott, P.H., Lawrence, J.C., Jr., and Roth, R.A. (1998). Construction and characterization of a conditionally active version of the serine/threonine kinase Akt. J. Biol. Chem. *273*, 11937–11943.

Kotani, K., Hara, K., Kotani, K., Yonezawa, K., and Kasuga, M. (1995). Phosphoinositide 3-kinase as an upstream regulator of the small GTP-binding protein Rac in the insulin signaling of membrane ruffling. Biochem. Biophys. Res. Commun. *208*, 985–990.

Koumanov, F., Jin, B., Yang, J., and Holman, G.D. (2005). Insulin signaling meets vesicle traffic of GLUT4 at a plasma-membrane-activated fusion step. Cell Metab. *2*, 179–189.

Lang, T., Wacker, I., Steyer, J., Kaether, C., Wunderlich, I., Soldati, T., Gerdes, H.H., and Almers, W. (1997). Ca2+-triggered peptide secretion in single cells imaged with green fluorescent protein and evanescent-wave microscopy. Neuron *18*, 857–863.

Li, C.H., Bai, L., Li, D.D., Xia, S., and Xu, T. (2004a). Dynamic tracking and mobility analysis of single GLUT4 storage vesicle in live 3T3-L1 cells. Cell Res. *14*, 480–486.

Li, D., Xiong, J., Qu, A., and Xu, T. (2004b). Three-dimensional tracking of single secretory granules in live PC12 cells. Biophys. J. *87*, 1991–2001.

Lizunov, V.A., Matsumoto, H., Zimmerberg, J., Cushman, S.W., and Frolov, V.A. (2005). Insulin stimulates the halting, tethering, and fusion of mobile GLUT4 vesicles in rat adipose cells. J. Cell Biol. *169*, 481–489.

Malide, D., Ramm, G., Cushman, S.W., and Slot, J.W. (2000). Immunoelectron microscopic evidence that GLUT4 translocation explains the stimulation of glucose transport in isolated rat white adipose cells. J. Cell Sci. *113*, 4203–4210.

Oatey, P.B., Van Weering, D.H., Dobson, S.P., Gould, G.W., and Tavare, J.M. (1997). GLUT4 vesicle dynamics in living 3T3 L1 adipocytes visualized with green-fluorescent protein. Biochem. J. *327*, 637–642.

Oh, E., and Thurmond, D.C. (2006). The stimulus-induced tyrosine phosphorylation of Munc18c facilitates vesicle exocytosis. J. Biol. Chem. *281*, 17624–17634.

Oheim, M., and Stuhmer, W. (2000). Tracking chromaffin granules on their way through the actin cortex. Eur. Biophys. J. *29*, 67–89.

Okada, T., Kawano, Y., Sakakibara, T., Hazeki, O., and Ui, M. (1994). Essential role of phosphatidylinositol 3-kinase in insulin-induced

glucose transport and antilipolysis in rat adipocytes. Studies with a selective inhibitor wortmannin. J. Biol. Chem. *269*, 3568–3573.

Robinson, L.J., Pang, S., Harris, D.S., Heuser, J., and James, D.E. (1992). Translocation of the glucose transporter (GLUT4) to the cell surface in permeabilized 3T3-L1 adipocytes: effects of ATP insulin, and GTP gamma S and localization of GLUT4 to clathrin lattices. J. Cell Biol. *117*, 1181–1196.

Saltiel, A.R., and Kahn, C.R. (2001). Insulin signalling and the regulation of glucose and lipid metabolism. Nature *414*, 799–806.

Saltiel, A.R., and Pessin, J.E. (2003). Insulin signaling in microdomains of the plasma membrane. Traffic *4*, 711–716.

Sano, H., Kane, S., Sano, E., Miinea, C.P., Asara, J.M., Lane, W.S., Garner, C.W., and Lienhard, G.E. (2003). Insulin-stimulated phosphorylation of a Rab GTPase-activating protein regulates GLUT4 translocation. J. Biol. Chem. *278*, 14599–14602.

Satoh, S., Nishimura, H., Clark, A.E., Kozka, I.J., Vannucci, S.J., Simpson, I.A., Quon, M.J., Cushman, S.W., and Holman, G.D. (1993). Use of bismannose photolabel to elucidate insulin-regulated GLUT4 subcellular trafficking kinetics in rat adipose cells. Evidence that exocytosis is a critical site of hormone action. J. Biol. Chem. *268*, 17820–17829.

Schmelzle, K., Kane, S., Gridley, S., Lienhard, G.E., and White, F.M. (2006). Temporal dynamics of tyrosine phosphorylation in insulin signaling. Diabetes *55*, 2171–2179.

Schmoranzer, J., Goulian, M., Axelrod, D., and Simon, S.M. (2000). Imaging constitutive exocytosis with total internal reflection fluorescence microscopy. J. Cell Biol. *149*, 23–32.

Semiz, S., Park, J.G., Nicoloro, S.M., Furcinitti, P., Zhang, C., Chawla, A., Leszyk, J., and Czech, M.P. (2003). Conventional kinesin KIF5B mediates insulin-stimulated GLUT4 movements on microtubules1. EMBO J. *22*, 2387–2399.

Sorensen, J.B. (2005). SNARE complexes prepare for membrane fusion. Trends Neurosci. *28*, 453–455.

Steyer, J.A., Horstmann, H., and Almers, W. (1997). Transport, docking and exocytosis of single secretory granules in live chromaffin cells. Nature *388*, 474–478.

Tengholm, A., and Meyer, T. (2002). A PI3-kinase signaling code for insulin-triggered insertion of glucose transporters into the plasma membrane. Curr. Biol. *12*, 1871–1876.

Thurmond, D.C., Gonelle-Gispert, C., Furukawa, M., Halban, P.A., and Pessin, J.E. (2003). Glucose-stimulated insulin secretion is coupled to the interaction of actin with the t-SNARE (target membrane soluble N-ethylmaleimide-sensitive factor attachment protein receptor protein) complex. Mol. Endocrinol. *17*, 732–742.

van Dam, E.M., Govers, R., and James, D.E. (2005). Akt activation is required at a late stage of insulin-induced GLUT4 translocation to the plasma membrane. Mol. Endocrinol. *19*, 1067–1077.

Watson, R.T., Khan, A.H., Furukawa, M., Hou, J.C., Li, L., Kanzaki, M., Okada, S., Kandror, K.V., and Pessin, J.E. (2004). Entry of newly synthesized GLUT4 into the insulin-responsive storage compartment is GGA dependent. EMBO J. *23*, 2059–2070.

Zenisek, D., Steyer, J.A., Feldman, M.E., and Almers, W. (2002). A membrane marker leaves synaptic vesicles in milliseconds after exocytosis in retinal bipolar cells. Neuron *35*, 1085–1097.